JOURNAL OF Applied Polymer SCIENCE

# Effect of the Type of Clay Organo-Modifier on the Morphology, Thermal/Mechanical/Impact/Barrier Properties and Biodegradation in Soil of Polycaprolactone/Clay Nanocomposites

**L. N. Ludueña,[1] A. Vázquez,[2] V. A. Alvarez[1]**

[1]Research Institute of Material Science and Technology (INTEMA, UNMdP-CONICET), Composite Materials Group (CoMP) Engineering Faculty, National University of Mar del Plata, Juan B. Justo 4302 (B7608FDQ) Mar del Plata, Argentina

[2]Institute of Engineering Science and Technology (INTECIN, UBA-CONICET), Polymer and Composite Group, Engineering Faculty, University of Buenos Aires, Las Heras 2214 (1127AAR) Buenos Aires, Argentina

Correspondence to: V. A. Alvarez (E-mail: alvarezvera@fi.mdp.edu.ar)

**ABSTRACT:** The effect of addition of unmodified (CNa+) and modified (C30B and C20A) montmorillonites on the performance of polycaprolactone (PCL) based nanocomposites prepared by melt intercalation was studied. The study covers morphological and thermal aspects, mechanical and barrier properties and also biodegradability, which are important for packaging applications. Particular effort was made to find the main characteristics of the clays responsible for the final clay dispersion degree inside the nanocomposite. The most hydrophobic reinforcement (demonstrated by water adsorption tests) also showed the strongest thermal stability (shown by thermogravimetrical analysis) and the larger basal spacing (calculated by X-ray diffractometry (XRD)), which were the main characteristics that led to the best clay dispersion degree inside the PCL matrix (demonstrated by XRD and Transmission Electron Microscopy (TEM)). The findings demonstrate that a biodegradable polymer/clay nanocomposite with enhanced mechanical, impact, and barrier properties was obtained. © 2012 Wiley Periodicals, Inc. J. Appl. Polym. Sci. 000: 000–000, 2012

**KEYWORDS:** nanocomposites; clay; biodegradable; impact resistance; barrier

Received 1 September 2011; accepted 24 July 2012; published online
**DOI: 10.1002/app.38425**

## INTRODUCTION

It is known that waste accumulation is actually a serious problem and, so that, the development of environmental friendly, degradable, polymeric materials has attracted extensive interest.[1] Within them, PCL is one of the best candidates.[2] PCL is a hydrophobic, biodegradable, and semicrystalline polyester. Its crystallinity tends to decrease with increasing molecular weight.[2–5] Its melting point and glass transition temperature are about 60°C and −60°C, respectively.[6,7] PCL can be processed using conventional plastics machinery[2,8] and their properties make them suitable for a number of potential applications from agricultural usage to biomedical devices.[9] Special interest is focused on packaging applications which is the biggest industry of disposable polymer products but until now, the relative high price and the weak rigidity of the PCL have limited their large-scale production as a substitute of traditional polymers.[10] To overcome the limitations of PCL, one of the cheapest environmental friendly and efficient options is to incorporate nanofillers, such us clays to produce nanocomposites. These hybrid materials can exhibit high improvements on the mechanical, barrier and thermal properties,[8,11,12] and some others such as the flammability,[13] water adsorption,[14] and creep resistance[15] with the incorporation of small amounts of filler (usually less than 10 wt %).[8,11–15] Moreover, higher filler contents reduce the price of the material, but it was demonstrated for several thermoplastic matrices that even when the silicate layers are exfoliated or intercalated in the polymer matrix, the particles begins to agglomerate at a clay content usually higher than 10 wt %, which reduce the efficiency of the filler as reinforcement.[1,8,16,17] Anyway, several procedures are widely known so far to incorporate layered silicate materials in a fine-dispersed manner into polymer matrix materials.[18] Chen et al.[19] were able to prepare intercalated PCL/clay nanocomposites with organo-modified montmorillonite contents up to 30 wt %. They also prepared microcomposites with 58.5 wt % of natural montmorillonite and suggests that it is not the largest clay loading that PCL with a molecular weight of 80,000 can sustain.

The most used nanoclay is the montmorillonite, a layered silicate whose interlayer cations can be exchanged by organ-cations in order to increase the interlayer spacing ($d_{001}$) and to improve

the polymer/clay compatibility allowing the easier intercalation of the polymer chains in between the silicate layers.[20]

Huge efforts have been done in order to improve the final properties of polymer/clay nanocomposites[18,21–26]; concluding that the enhancements are related with two main parameters: the clay content and the clay dispersion degree inside the matrix.

PCL/clay nanocomposites with enhanced clay dispersion degree as a function of the clay surface hydrophobicity and its initial clay interlayer distance are expected to be obtained. Conversely, several authors obtained the opposite tendencies.[1,4,27] Janigová et al.[27] prepared PCL/clay nanocomposites by melt blending. Natural montmorillonite and two montmorillonite clays modified with dimethyl, benzyl, hydrogenated tallow, quaternary ammonium (2MBHT) and dimethyl, dehydrogenated tallow, quaternary ammonium (2M2HT) were used as fillers. It must be mentioned that the supplier of the clays (Southern clay products) recommends an initial screening for the selection of their Cloisite® products relative to the hydrophobicity/hydrophilicity hydrophobic/hydrophilic nature of the system. The authors of this work demonstrated by TEM and XRD lower dispersion degree for PCL/Cloisite® 15A nanocomposites and almost the same Young's modulus than PCL/Cloisite 10A® nanocomposites. They did not analyze the effect of the PCL/clay hydrophobicity/hydrophilicity nature and the initial clay interlayer distance on these results but it can be observed on the web page of the supplier that Cloisite® 15A is more hydrophobic and has higher interlayer distance than Cloisite 10A®, so, the results were opposite as those expected. The same tendencies were obtained by Zheng et al.[4] and Lepoittevin et al.[1] for PCL based nanocomposites prepared by melt blending using Cloisite® 30B and Cloisite® 15A[4]; and Cloisite® 30B and Cloisite® 25A,[1] respectively, as fillers. In both works they obtained the highest clay dispersion degree with PCL/Cloisite® 30B nanocomposites and they did not find substantial differences in the mechanical properties between the different nanocomposites even when Cloisite® 15A and Cloisite® 25A are more hydrophobic and have larger interlayer distance than Cloisite® 30B. Chen et al.[28] prepared PCL/clay nanocomposites by melt processing. They used natural sodium montmorillonite from Blackhill Bentonite LLC and two montmorillonite clays modified with benzyl-2-methyl-hydrogenated tallow quaternary ammonium chloride (NH4MMT2) and 2-methyl-2-hydrogenated tallow quaternary ammonium chloride (NH4MMT1) from Elementis Specialties, which are the same modifiers as those used in Cloisite® 10A and Cloisite® 20A, respectively. It was proved by XRD that the interlayer distance of NH4MMT2 was lower than that of NH4MMT1. On the other hand, the hydrophobicity/hydrophilicity nature of the system was not analyzed but the available information about Cloisite® 10A and Cloisite® 20A suggests that NH4MMT1 is more suitable as filler of PCL than NH4MMT2. Even so, the nanocomposites prepared with NH4MMT2 showed the highest clay dispersion degree and led to the greater enhancement of the Youngs modulus of the PCL at low filler loading. As a first approach to understand these results, we analyzed previous studies[1,14,20,23,29] which concluded that the dispersion degree achieved in the preparation of polymer/clay nanocomposites depends not only on the initial clay basal spacing and the chemical compatibility of the system, but also on the processing technique and conditions. A possible explanation for these results can be found in the works carried out by VanderHart et al.[30,31] who demonstrated by nuclear magnetic resonance (NMR) that a considerable portion of the alkyl quaternary ammonium compound (which was the organo-modifier of the clay) is removed during the preparation of nylon 6 nanocomposites by melt mixing. They concluded that the main reason for the degradation is the combination of the temperature with shear forces developed during mixing.

Based on the reviewed literature, we concluded that the degradation of the clay organo-modifiers during melt blending is not possible to be quantified and depends on several variables such as the processing stability of the modifier itself, the matrix used, the processing technique and the processing parameters used. Furthermore, the clay loading after mixing (considered as the sum of the weight of silicate layers and the residual weight of the organo-modifier) can be lower than that weighed before the process. Therefore, the hypothesis of this work is that the clay that shows the highest interlayer distance and meets the optimal filler/matrix hydrophobicity/hydrophilicity balance may lead or not to the best dispersed nanocomposite with the most efficiently enhanced properties depending on the processing stability of the clay organo-modifiers. Thus, the aim of this article is to demonstrate this hypothesis analyzing the effect of the clay hydrophobicity, the initial clay interlayer distance and the thermal stability of the clay organo-modifiers on the final clay dispersion degree, thermal, tensile, barrier, and impact properties and the biodegradation in soil of PCL/clay nanocomposites. For this purpose, natural montmorillonite and two modified montmorillonite clays will be characterized by water absorption, thermogravimetrical analysis and X-ray diffractometry.

## EXPERIMENTAL

### Materials

The matrix used in this work was a commercial polycaprolactone ($M_n$ 80,000), supplied by Sigma Aldrich. Three Cloisite® clays commercially purchased from Southern Clay Products, USA, were used as nanofillers. They were used as received. The characteristics of the clays are shown in Table I.

### Nanocomposites Preparation

Matrix and nanocomposites with 5 wt % of each filler were prepared in a double-screw mini-extruder *DSM Xplore 5&15 microcompounder* using a temperature profile of: 60–90–120°C at a rotating rate of 150 rpm; the residence time was 1 min. Then, films were obtained by compression molding (100°C, 10 min without pressure and 10 min at 50 bar, the molds were water-cooled). The different compression molded films were named as PCL for the neat matrix and PCL/CNa+, PCL/C30B, and PCL/C20A for the nanocomposites.

### Methods

XRD patterns of clays and nanocomposites were recorded by a PW1710 diffractometer equipped with an X-ray generator ($\lambda$ = 0.154060 nm). Samples were scanned in 2θ ranges from 3° to 60° by a step of 0.035°. The interlayer spacing of clays was calculated before and after mixing by means of the Bragg's Law.

**Table I.** Characteristic of Clays Used as Nanofillers

| Clay | Organic modifier | Modifier content (wt %) | Specific gravity (g/cm$^3$) | $d_{001}{}^{initial}$ (Å) | $M_{24}$ (%) | Water content (%)[c] |
|---|---|---|---|---|---|---|
| Montmorillonite (CNa+) | None | - | 2.86 | 14.0 | 13.0 | 9.9 |
| Closite 30B (C30B) | 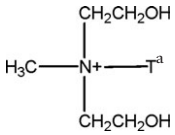 | 28 | 1.98 | 18.8 | 4.4 | 2.2 |
| Cloisite 20A (C20A) | 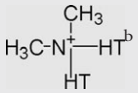 | 40 | 1.77 | 24.2 | 3.7 | 1.8 |

[a]T is Tallow (~65% C18; ~30% C16; ~5% C14), [b]HT is Hydrogenated Tallow (~65% C18; ~30% C16; ~5% C14), [c]Calculated from thermogravimetrical analysis.

This parameter was named $d_{001}{}^{initial}$ (before melt blending) and $d_{001}{}^{final}$ (after melt blending).

Water absorption tests of the clays were carried out at 90% RH (simulated from a solution of 34 wt % of glycerin). Before tests, all the samples were dried under vacuum until constant weight. Samples were weighed at prefixed times and the absorption at each time was calculated as:

$$M_t(\%) = \frac{M_t - M_0}{M_0} \times 100 \quad (1)$$

where $M_t$ is the mass of the sample at a time $t$ and $M_0$ is the initial mass of the sample (dried).

Thermogravimetric analysis (TGA) was carried out in a Shimadzu TGA-50 from 30 to 1000°C at 10°C/min. Tests in nitrogen atmosphere were done for clays alone, in order to calculate the content of water and the content of organo-modifiers (Table I); and for nanocomposites, to estimate the clay content inside the nanocomposites. The content of water within the filler was calculated from the residual mass of the clays at 120°C. The content of organo-modifiers was calculated from the residual mass of the clays at 900°C correcting for the water content. The clay amount inside the nanocomposites was calculated from the residual mass of the composites at 900°C correcting for the residual mass of the neat matrix and for the weight loss of the clays at the same temperature. Then, tests in air atmosphere were performed for the clays in order to determine the degradation temperature of the organic modifiers in conditions similar to those used for melt blending.

Transmission electron microscope (TEM) micrographs of the nanocomposites were taken by a JEOL JEN 1220 operated at 100 kV in the bright field mode. Ultrathin sections (~50 nm) of the samples were cut at −120°C using a Leica UCT ultramicrotome equipped with a diamond knife.

Tensile tests were performed in a universal testing machine Lloyd Instruments LR30K at a constant crosshead speed of 50 mm/min. Before tests, all specimens were preconditioned at 65% RH (relative humidity) at room temperature. Four samples of each material were tested.

Differential Scanning Calorimetry (DSC) tests were performed in a Shimadzu DSC-50 from 25 to 100°C at a heating rate of 10°C/min under nitrogen atmosphere (ASTM D3417-83). The degree of crystallinity was calculated from the following equation:

$$X_{cr}(\%) = \frac{\Delta H_f}{w_{PCL} \times \Delta H_{100}} \times 100 \quad (2)$$

where $\Delta H_f$ is the experimental heat of fusion, $w_{PCL}$ the PCL weight fraction and $\Delta H_{100}$ is the heat of fusion of 100% crystalline PCL (136.1 J/g[32]).

The same equipment was used to calculate the glass transition temperature ($T_g$) of the neat matrix and nanocomposites. The tests were carried out from −105 to 100°C at 10°C/min under nitrogen atmosphere. The lower temperature was reached cooling the DSC chamber with liquid nitrogen. The $T_g$ value was calculated following the midpoint method of the ASTM D-3418-99 standard.

Impact tests; puncture tests were conducted on 30-mm-diameter samples cut out from molded film. These tests were performed in a falling weight Fractovis Ceast at 1 m/s. From these tests, load–displacement curves were obtained. The total energy required to fully penetrate the specimen, $E_{tot,}$ was calculated as the total area under the load–displacement curve normalized by the sample thickness.

Water Vapor Transmission (WVT) was determined by following the ASTM E96-00 recommendations by using the Desiccant Method ($CaCl_2$). The films were preconditioned in a chamber at 68% RH at room temperature until reaching equilibrium conditions (2 days). A fan was used to maintain the air continuously circulated throughout the chamber in order to ensure uniform conditions at all test locations. After that, dehydrated Calcium Chloride ($CaCl_2$) was placed in the low chamber of an acrylic cup sealed by the samples. Thus, the corresponding RHs were 0% inside the cup and 68% outside of the cup. The RH difference promotes a pressure gradient for the vapor transmission. The weights of the assembled cups were recorded every 12 h for 10 days. Weight versus time was plotted for each

sample and fitted by linear regression in order to calculate the slope of the resulting line. Water vapor permeability values were reported as WVP $(g \cdot m/Pa \cdot s \cdot m^2)$ which is calculated as follows:

$$\mathrm{WVP} = \frac{\Delta W}{\Delta t} \cdot y \cdot [A \cdot (p_2 - p_1)]^{-1} \quad (3)$$

where $\Delta W/\Delta t$ is the calculated slope (weight of water absorbed by the cup/time interval, g/s); $y$ is the film thickness, $A$ is the exposed area of the film and $p_2 - p_1$ is the vapor pressure difference across the film, which is calculated on the basis of the RH and temperature inside and outside the cup. Three samples of each material were tested in order to ensure the reproducibility of the results.

Indoor soil burial experiments were carried out as reported by Di Franco et al.[33] Basically, a series of plastic boxes (30 cm × 15 cm × 10 cm) were used as soil containers. Natural microflora present in soil (Pinocha type) was used as the degrading medium. Several specimens (rectangular shape, 10 mm × 20 mm × 0.3–0.5 mm) of PCL and nanocomposites obtained from films were put into cups made of an aluminum mesh to permit the access of microorganisms and moisture and the easy retrieval of the degraded samples. The specimens into the holders were buried at a depth of 8 cm from the surface in order to ensure the aerobic degradation. The average room temperature was 20°C and relative humidity was kept around 40% by adding distilled water. Samples were removed from the soil at specific intervals ($t$), carefully cleansed with distilled water and superficially dried. After that, samples were dried under vacuum at 35°C until constant weight. The specimens were weighed on an analytical balance in order to determine the average weight loss (%WL):

$$\mathrm{WL} = \frac{w_0 - w_t}{w_0} \times 100 \quad (4)$$

where $w_0$ is the initial mass and $w_t$ is the remaining mass at time $t$. All results are the average of two replicates.

## RESULTS AND DISCUSSIONS

### Clays Characterization

In this section, the main factors that control the final clay dispersion degree in the nanocomposites will be analyzed. Table I shows the interlayer distance ($d_{001}{}^{\mathrm{initial}}$) of the nanoclays calculated by XRD. The highest value was found for the C20A clay. It is supposed that the higher the $d_{001}{}^{\mathrm{initial}}$ value, easier the intercalation of the polymer chains into the silicate layers.[18] Another main factor is the hydrophobic/hydrophilic nature of the system. The PCL matrix is hydrophobic with a very low degree of polarity; around 6%,[34] therefore it is expected higher interaction with the less hydrophilic filler, as is also suggested by the clay supplier. In this work, the degree of polarity of the clays was compared by moisture absorption tests, which provides information about the surface and bulk hydrophilicity of the material. Figure 1 shows the results of water absorption as a function of time ($M_t$) and Table I resumes the values after 24 h ($M_{24}$). It can be seen in Figure 1 that the unmodified clay

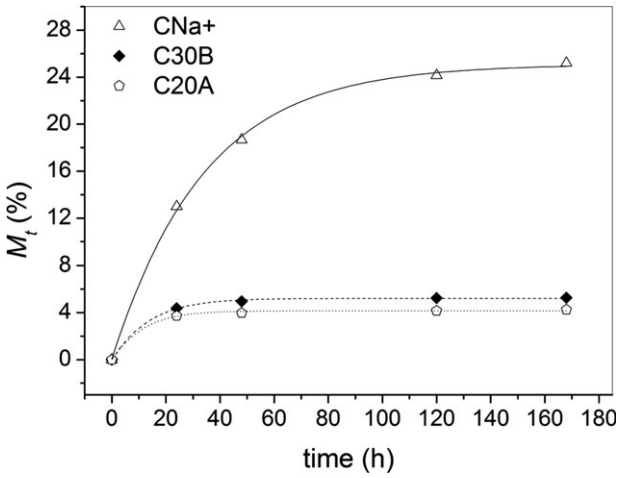


**Figure 1.** Water absorption of the clays as a function of time.

(CNa+) reached the equilibrium at longer times than the modified ones (C30B and C20A). It can be attributed to the lower interlayer distance of CNa+ that delays the access of the water molecules into the galleries. On the other hand, the water content at equilibrium ($M_{24}$) was substantially higher for CNa+ than for C30B and C20A due to the lower water affinity of the organo-modifiers in comparison with the sodium cations of CNa+. Comparing the two organo-modified clays, both reached the equilibrium at the same time but C20A presented the lowest $M_{24}$ value. It can be attributed to the OH-groups of the C30B organo-modifiers that can easily form hydrogen bonds with the water molecules. From these results, it can be concluded that C20A is the most hydrophobic clay and so it is a potential candidate as reinforcement of hydrophobic polyesters such as PCL. Even so, as was previously explained in the introduction, the processing stability of the organic-modifiers of the clays can be decisive to obtain the expected clay morphology when the nanocomposites are prepared by means of intense shear and temperature, as those involved in a twin-screw extruder.[35] Figure 2(a, b) shows the residual mass of clay as a function of temperature and the DTGA analysis in air atmosphere, respectively. The peaks shown in Figure 2(b) indicate the maximum speed of thermal degradation. It can be observed from Figure 2(a) that the clay CNa+ has a steep drop in residual mass in the range of 50–120°C due to evaporation of water from the sample, showing that this reinforcement has the greater hydrophilic character (as was also shown in Figure 1). Table I summarizes the water content of each clay calculated from TGA. It can be observed that the values are consistent with those from the water adsorption tests: as stronger the hydrophilicity, higher the water content is. It can be noted from Figure 2(b) that the initial degradation temperature ($T_{\mathrm{initial}}$) and the temperature at the maximum speed of thermal degradation ($T_{\mathrm{peak}}$) of the organic-modifiers were 150 and 265°C for C30B, and 190 and 307°C for C20A. Table I shows that the content of organic-modifier on the total mass of clay is 28 wt % for C30B and 40 wt % for C20A, therefore, it is crucial to consider their degradation during processing because if it happens, not only the final dispersion degree of the clay inside the nanocomposite can be affected, but also the final clay content inside the matrix which

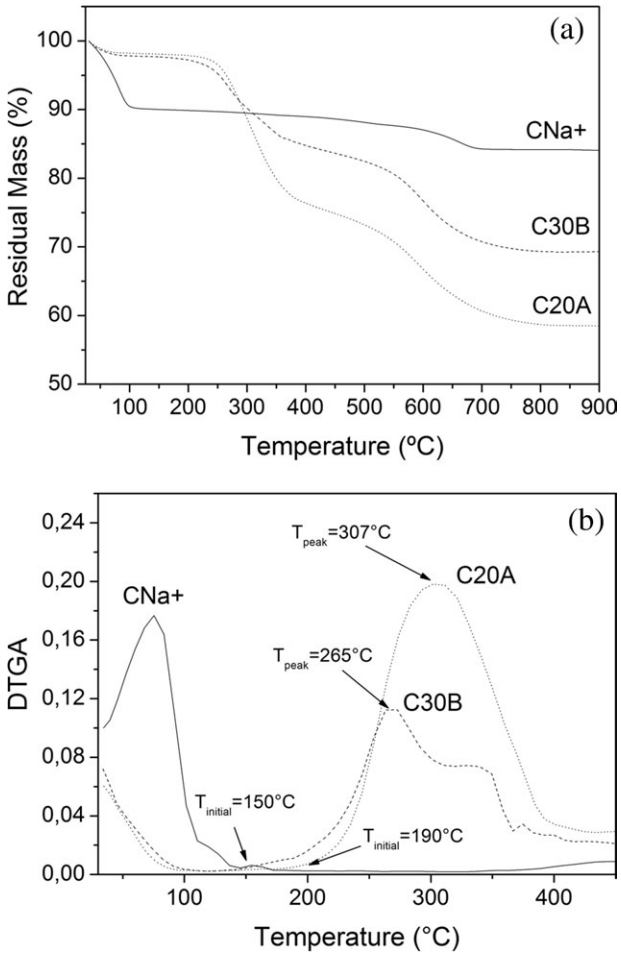


**Figure 2.** Thermogravimetrical analysis of the clays: (a) residual mass as a function of temperature (TGA); (b) derivative of the residual mass as a function of temperature (DTGA).

can be lower than that introduced in the extruder. In our case, the processing temperature of the extruder barrel did not exceed 120°C, but it is well known that the shear forces developed in the mixer, together with the high viscosity of the polymer, increase the melt temperature by viscous dissipation; therefore, the clay modifiers may have degraded in different proportions, depending on the characteristics of each one.

In conclusion, the C20A clay showed the highest hydrophobicity, the larger interlayer distance and the strongest thermal stability, therefore, based on the hypothesis of this work, PCL/

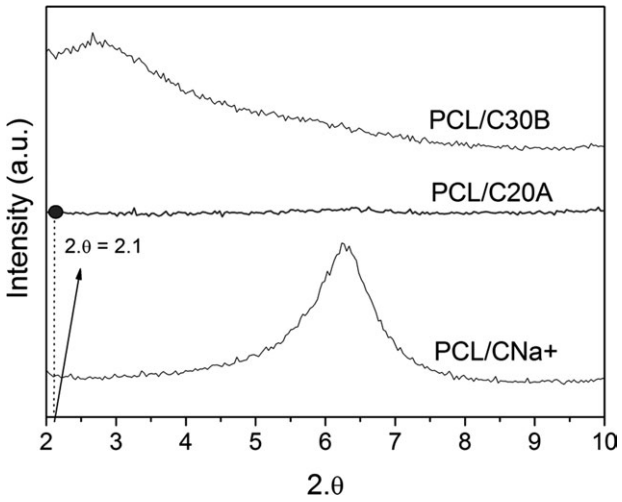


**Figure 3.** XRD patterns for the PCL/clay nanocomposites.

C20A nanocomposites prepared by melt mixing should show the best clay dispersion degree, and hence, improved mechanical and barrier properties.

### Nanocomposites Characterization

**Morphology.** The degree of dispersion of the clay inside the matrix was studied by XRD and TEM. Figure 3 shows the XRD patterns for the nanocomposites. In the case of PCL/CNa+ and PCL/C30B the peak corresponding to the clay interlayer distance was identified. In the case of PCL/C30B this peak shifted to lower angles than that of PCL/CNa+ which indicates a higher extent of intercalation of the polymer chains into the C30B galleries. On the other hand, for PCL/C20A the peak disappeared indicating that the interlayer distance of the intercalated layers is so long that the resolution of the equipment is not enough to identify it, or that the nanocomposite does not present ordering anymore (exfoliation). From the 2.θ values of the basal peaks and using the Bragg's Law, the interlayer distance of the clays inside the nanocomposites ($d_{001}{}^{\text{final}}$) was calculated. Using the $d_{001}{}^{\text{initial}}$ and $d_{001}{}^{\text{final}}$ values the increment of the interlayer distance can be calculated by the following equation:

$$\Delta d_{001} = (d_{001}^{\text{final}} - d_{001}^{\text{initial}})/d_{001}^{\text{initial}} \times 100 \quad (5)$$

This parameter can be thought as a quantitative measure of the efficiency of the intercalation of the polymer chains between the

**Table II.** Parameters Obtained from Morphological Analysis (XRD) and Mechanical, Impact, Thermal, and Permeability Measurements for the Neat Matrix and Their Nanocomposites

| Material | $d_{001}{}^{\text{final}}$ (Å) | $\Delta d_{001}$ (%) | Modulus (MPa) | Strength (MPa) | Elongation at break (%) | $E_{\text{tot}}$ (J/m) | $X_{\text{cr}}$ (%) | $T_g$ (°C) | WVP [g/(s.m.Pa)]$^a 10^{-11}$ |
|---|---|---|---|---|---|---|---|---|---|
| PCL | - | - | 233 ± 7 | 15.0 ± 0.3 | 1906 ± 82 | 926 | 72 | −63 | 2.03 ± 0.10 |
| PCL/CNa+ | 14.1 | 21 | 240 ± 8 | 15.8 ± 1.3 | 1345 ± 123 | 1095 | 68 | −64 | 1.79 ± 0.06 |
| PCL/C30B | 33.1 | 79 | 303 ± 28 | 14.0 ± 0.2 | 1212 ± 38 | 1197 | 72 | −63 | 1.30 ± 0.03 |
| PCL/C20A | 43.3[a] | - | 331 ± 30 | 14.1 ± 0.9 | 1430 ± 35 | 1259 | 71 | −63 | 1.21 ± 0.10 |

[a]Conservative value. It was calculated based on the $\Delta d_{001}$ for PCL/C30B using eq. (5).

Applied Polymer SCIENCE

silicate layers. The $d_{001}{}^{final}$ and $\Delta d_{001}$ values are reported in Table II. The position of the 2θ diffraction peak for PCL/C20A was calculated by means of eq. (5) and the Bragg's Law in the hypothetical case that this nanocomposite shows the same $\Delta d_{001}$ value as that of PCL/C30B. The position was $2\theta = 2.1^{\circ}$ but it can be seen in Figure 3 that no peak is present for PCL/C20A at that position, marked with a black dot in the figure, which confirms that the value of $\Delta d_{001}$ of PCL/C20A was even greater than that of PCL/C30B. A conservative value for $d_{001}{}^{final}$ was calculated for PCL/C20A by means of eq. (5) using the $\Delta d_{001}$ value of PCL/C30B (Table II). Figure 4(a–c) shows the TEM pictures for the nanocomposites. This technique can be used in order to observe the clay platelets structure; which are distinguished by the dark zones. Agglomerates (400–1000 nm) together with intercalated zones are present in the case of PCL/CNa+, whereas more intercalation is observed for PCL/C30B and even higher dispersion can be concluded for PCL/C20A, in accordance with XRD results.

**Mechanical Properties.** Table II summarizes the mechanical properties of the matrix and their nanocomposites. All the clays enhanced the Youngs modulus of the neat matrix while the tensile strength remained almost constant and the elongation at break decreased in the range of 25–36% in all cases. Such detriment on the elongation at break is not important taking into account that the value for the pure PCL was around 1900% while the values for commodities such as polypropylene, polystyrene, and polyethylene are around 50%.[36] Therefore, the main issue of the PCL (its low rigidity) was overcome maintaining the tensile strength and elongation at break at acceptable values. Figure 5 shows the Youngs modulus as a function of the clay dispersion degree represented by $d_{001}{}^{final}$. It can be observed an increasing trend of the Youngs modulus as a function of the clay dispersion degree which has been also demonstrated by several works regarding PCL/clay nanocomposites.[1,27,28] The Youngs modulus values are also consistent with those reported by Lepoittevin et al.[1] for PCL/CNa+ and PCL/C30B. The degree of crystallinity ($X_{cr}$) of the matrix is a property that also influences the mechanical properties of the material. Therefore, it is important to analyze the effect of the nanoclays on $X_{cr}$. Table II shows the crystallinity degree for PCL and their nanocomposites. For each material, the dispersion in values was negligible (less than 1%). It can be seen that the different materials have almost the same $X_{cr}$ value which indicates that it had not any effect on the mechanical properties tendencies. Labidi et al.[37] found a similar results for PCL reinforced with three different modified clays.

### Impact Behavior

Figure 6 shows the load-displacement curves obtained from impact tests of PCL and the nanocomposites PCL/CNa+, PCL/C30B, and PCL/C20A.

It can be observed that in all cases the curves increase with displacement until a peak, which delimits an area known as the energy required to initiate a crack. After this point, it can be seen (also in all the curves) that although the load begins to decrease with displacement, it does not abruptly, showing that energy is absorbed during the crack propagation. The area after

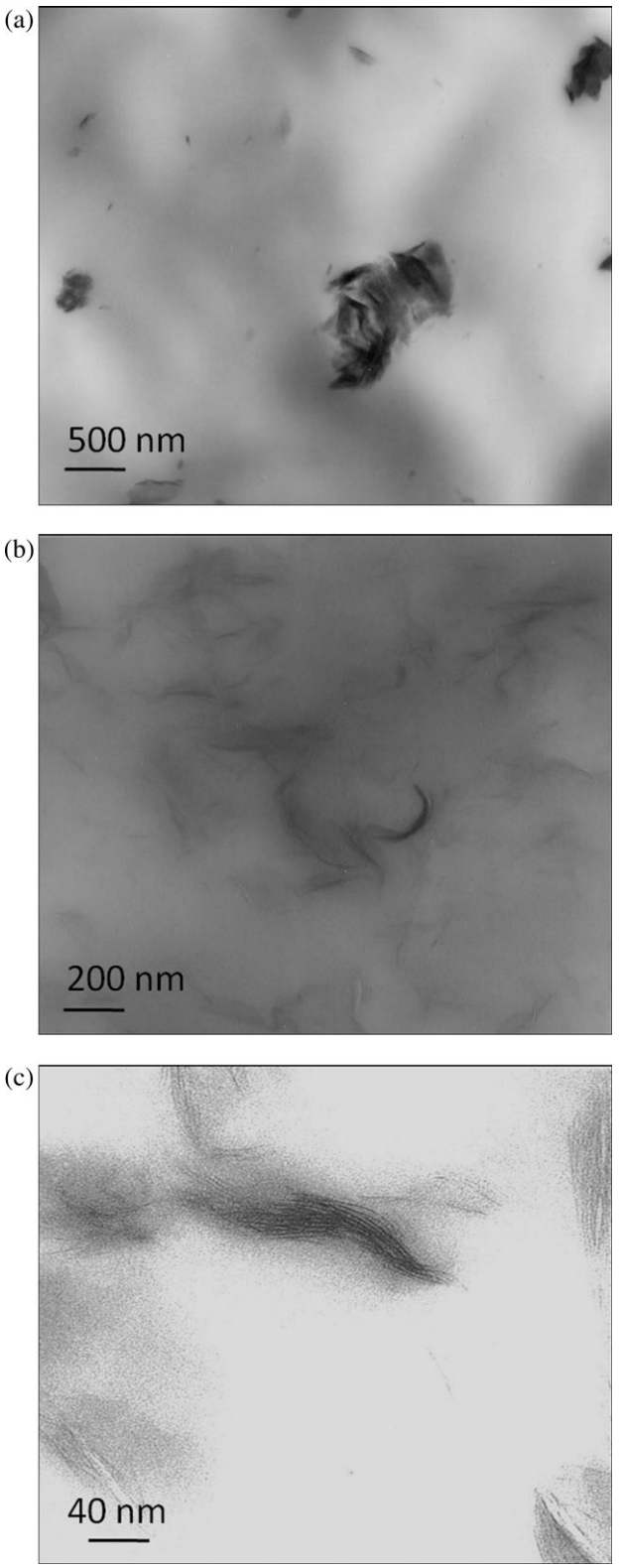


**Figure 4.** Transmission electron microscopy (TEM) micrographs of PCL based nanocomposites: (a) PCL/CNa+; (b) PCL/C30B, and (c) PCL/C20A.

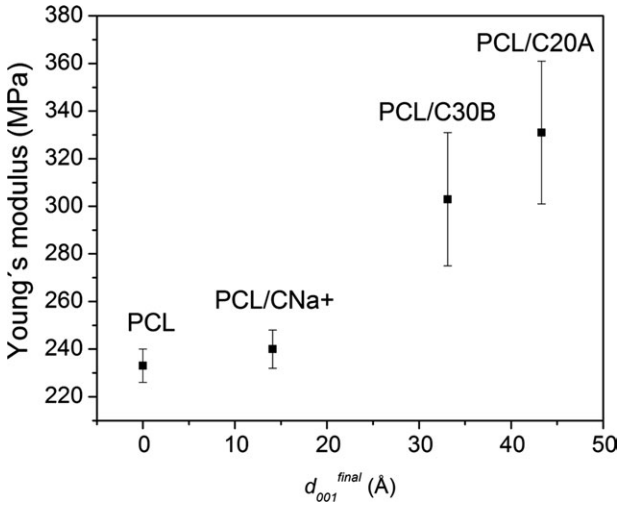


**Figure 5.** Youngs modulus as a function of $d_{001}^{final}$ for PCL and their nanocomposites.

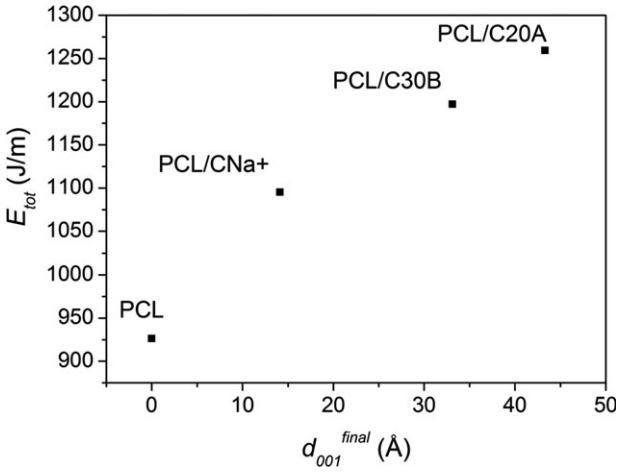


**Figure 7.** Impact energy as a function of $d_{001}^{final}$ for PCL and their nanocomposites.

the peak is known as the energy required to propagate a crack ($E_{prop}$). This behavior is typical for polymers that exhibit a ductile failure mechanism.[38] Table II summarizes the total energy values, $E_{tot,}$ of PCL and nanocomposites. The incorporation of all clays increased the fracture energy, suggesting that the clay provides mechanisms of damage that absorb energy during the impact fracture[39]. It can be observed from Figure 7 an increasing trend of $E_{tot}$ as a function of the clay dispersion degree, the latter represented by $d_{001}^{final}$. Sun et al.[39] have extensively reviewed the energy absorption mechanisms for polymer nanocomposites including several examples of polymer/clay nanocomposites concluding that when the dimensions of the strengthening particles approach the nanometer scale, the energy absorption mechanisms are more efficient and the corresponding properties of the compounds are different than those reinforced with equal amounts of macro and micro reinforcements. The main reason for these observations lies on the structure of the polymer/nanofiller interphase which is thicker and has higher shear strength than in conventional composites. So

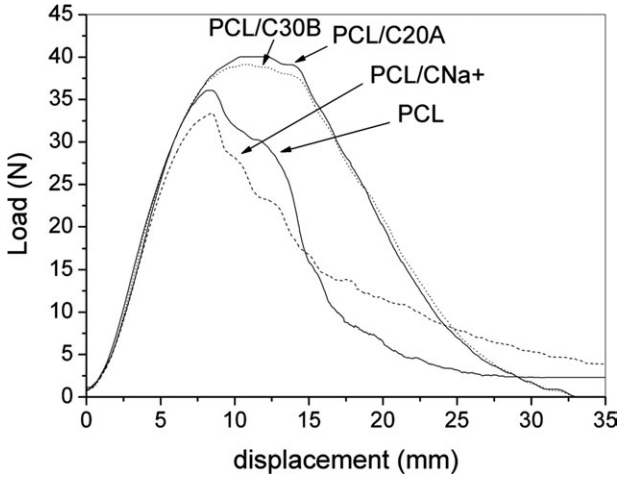


**Figure 6.** Load-displacement curves obtained in dart drop impact tests for the PCL and their nanocomposites.

that, for a given volume fraction, the large specific surface area of nanofillers, and the high nanofiller/matrix tensile strength ratio lead to greater pull-out energy and fracture energy for nanocomposites compared with conventional microfiller reinforced composites, but effective methods for avoiding nanofiller clustering are needed to maximize nanocomposites performance. In the case of PCL/clay nanocomposites, the only work found in the literature regarding this topic was the study reported by Lepoittevin et al.[1] who, conversely to the hypothesis above mentioned, showed that the Izod impact strength of the PCL is reduced as a function of the filler content when it is blended with natural and organo-modified montmorillonites (Cloisite® $Na^+$, Cloisite® 30B and Cloisite® 25A). The effect was more notorious for the nanocomposite that showed the highest clay dispersion degree, in contrast to the results reported in this work.

According to Galeski[40] changes in the glass transition temperature, $T_{g,}$ and the degree of crystallinity, $X_{cr,}$ of the matrix also influence the impact behavior of polymeric materials. It can be seen in Table II that the values of the different nanocomposites were in the range of $-63.5°C \pm 0.5°C$ and $70\% \pm 2\%$ for $T_g$ and $X_{cr,}$ respectively. These parameters did not significantly change by the incorporation of the clays; therefore, it can be assumed that the $T_g$ and $X_{cr}$ values of the matrix had not any effect on the impact properties tendencies.

**Permeability Tests.** The polymer/clay nanocomposites are effective for use as barrier materials for packaging in the food industry where the gas permeability determines the particular application of the material.[41] Incorporating small amounts of clay to the matrix (<5% by weight) have demonstrated improvements in gas barrier properties to various polymers such as polyimide,[42,43] polycaprolactone,[44] and polyvinyl alcohol.[45] Table II summarizes the results of the water vapor permeability tests for PCL and its nanocomposites PCL/CNa+, PCL/C30B, and PCL/C20A. It can be seen that the water vapor permeability decreased when CNa+ was incorporated to the PCL matrix. In addition, the changes became more pronounced for modified clays (C30B and C20A). The decreasing trend of WVP as a function of the degree of dispersion is clear in Figure 8. It has

Applied Polymer SCIENCE

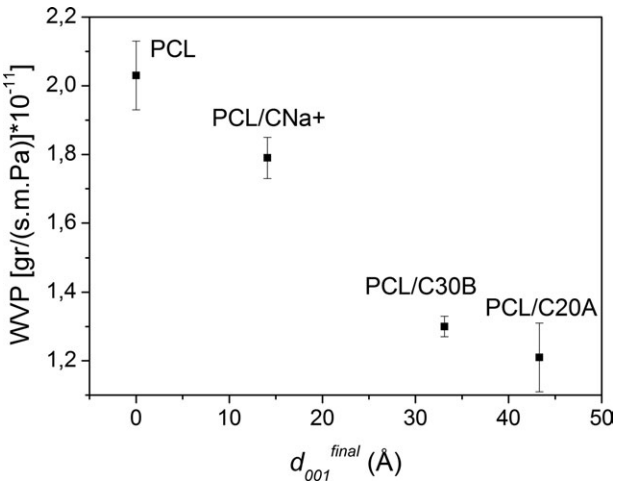


**Figure 8.** Water vapor permeability as a function of $d_{001}^{final}$ for PCL and their nanocomposites.

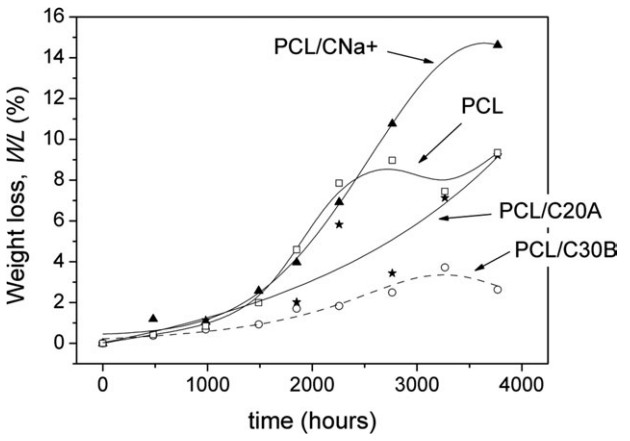


**Figure 9.** Weight loss as a function of time from biodegradation in soil tests for PCL and their nanocomposites.

been widely demonstrated that a high degree of dispersion of clay in a polymer matrix, including PCL, further improves the barrier properties compared with conventional microcomposites.[41–45] In addition, we demonstrated in this work that this conclusion is also related with the initial basal spacing of the clay, the hydrophobic/hydrophilic nature of the system and the processing stability of the clay organo-modifiers, which were optimized using C20A as filler.

**Biodegradation (Burial in Soil).** Table III shows photographs of samples from environmental degradation (Pinocha type soil, room temperature, 40% RH) at different times for the pure matrix and nanocomposites reinforced with CNa+, C30B, and C20A. It can be seen that from the 6th month the weight loss values increased considerably. At that time some fragments of the samples were separated from the specimens by the action of the advanced process of biodegradation and they could not be recovered for weighing. Therefore, the evolution of weight loss as a function of time was plot up to 5 months in Figure 9. From this figure it is not possible to identify the dependence of the weight loss as a function of time with any characteristic of the clay (such as the hydrophobicity, initial basal spacing or

**Table III.** Optical Photographs of Biodegradation in Soil as a Function of Time for the Matrix and Their Nanocomposites (20 mm)

| Material | Initial | 2 months | 4 months | 6 months | 8 months |
|---|---|---|---|---|---|
| PCL | WL = 0.0% | WL = 2.0% | WL = 9.0% | WL = 22.0% | |
| |  |  |  |  |  |
| PCL/CNa+ | WL = 0.0% | WL = 2.6% | WL = 10.8% | WL = 41.5% | |
| |  |  |  |  |  |
| PCL/C30B | WL = 0.0% | WL = 0.9% | WL = 2.5% | WL = 15.3% | |
| |  |  |  |  |  |
| PCL/C20A | WL = 0.0% | WL = 1.1% | WL = 3.4% | WL = 51.9% | |
| |  |  |  |  |  |

processing stability) nor the nanocomposite (such as the clay dispersion degree). Even so, in the case of the C30B nanocomposite, the results are in accordance with the work by Fukushima et al.[46] whom observed that the incorporation of C30B slows the rate of degradation of the polymer attributing this fact to the presence of the reinforcement that can hinder the access of the microorganisms to attack the ester groups $(-\overset{O}{\overset{\|}{C}}-O-)$ of PCL. On the other hand, Wu et al.[47] have found that the presence of unmodified montmorillonite nanoparticles delay the biodegradation process in composting of the PCL and more as a function of filler content, while the opposite result was obtained in this work as can be observed for the CNa+ nanocomposite in Figure 9. In addition, Ratto et al.[48] have found that several modified clays accelerate the process of degradation in soil of the PCL while in our case the C20A clay did not show any effect on the biodegradation process of PCL. On the other hand, Singh et al.[49] studied the biodegradability of pure PCL and its nanocomposites with two organo-modified clays including Cloisite C30B under controlled conditions in enzyme, pure microorganism (fungi), compost and Ganges water, finding that the rate of biodegradation dramatically increases by clay incorporation as a result of varying crystallinity and depolymerase activity at different pH arising out of clay incorporation in the matrix. They also found that the biodegradation rate depends strongly on the media used and that the presence of microorganism is a precondition to initiate biodegradation of PCL. Finally, they proposed that the biodegradation rate can be fine-tuned either by the incorporation of nanoclays (to increase the biodegradation rate) or changing the processing conditions to increase the crystallinity of the matrix (to decrease the biodegradation rate). The findings and conclusions of all these works are subject to precise experimental data and they are consistent with the stages of the degradation process for PCL but they show dissimilar results for similar PCL/clay systems which in some cases may arise from different preparation processes. In our case, more experimental work is needed to deeply understand the biodegradation process of the systems studied but the aim of this work was to analyze the effect of the nanoclays on this process focusing on disposable packaging applications for which long service life is needed but short degradation times in landfill burial sites are desired. The long service life can be guaranteed from the results obtained by Singh et al.,[49] who found that the presence of microorganisms (usually not present in service) is a precondition to initiate biodegradation of PCL, while short degradation times of samples buried in soil where shown in this work.

## CONCLUSIONS

PCL/clay nanocomposites films were successfully prepared by melt intercalation in a double screw extruder followed by compression molding. The results obtained suggest that the main characteristics responsible on the final morphology and properties of the PCL/clay nanocomposites are the hydrophobic/hydrophilic nature of the system, the initial basal spacing of the clay and the processing stability of the clay organo-modifiers. It was experimentally demonstrated that C20A meets the optimal combination of these parameters for preparing PCL based nanocomposites. As a consequence of this result, PCL/C20A nanocomposites displayed the best clay dispersion degree and showed improvements in several properties strategically studied focusing in packaging applications: the Youngs modulus increased 42%, the total energy absorbed in puncture impact tests increased 36% and the water vapor permeability decreased 40%. Moreover, it was demonstrated that the biodegradation behavior in soil of this nanocomposite makes it a potential candidate for the replacement of commodities in disposable polymer packaging applications. In future works we plan to chemically modify Argentinian bentonite clays with more stable cations expecting to obtain a cheaper product with stronger processing stability than C20A. The morphology and final properties of PCL based nanocomposites reinforced with these fillers will be analyzed studying also the effect of clay content.

## ACKNOWLEDGMENTS

Authors acknowledge to Mincyt, UNMdP, and CONICET for the financial support.

## REFERENCES

1. Lepoittevin, B.; Devalckenaere, M.; Pantoustier, N.; Alexandre, M.; Kubies, D.; Calberg, C.; Jérôme, R.; Dubois, P. *Polymer* **2002,** *43*, 4017.
2. Kunioka, M.; Ninomiya, F.; Funabashi, M. *Polym. Degrad. Stabil.* **2007,** *92*, 1279.
3. Homminga, D.; Goderis, B.; Hoffman, S.; Reynaers, H.; Groeninckx, G. *Polymer* **2005,** *46*, 9941.
4. Zheng, X.; Wilkie, C. A. *Polym. Degrad. Stabil.* **2003,** *82*, 441.
5. Morin, A.; Dufresne, A. *Macromolecules* **2002,** *35*, 2190.
6. Sinha Ray, S.; Bousmina, M. *Prog. Mater. Sci.* **2005,** *50*, 962.
7. Marras, S. I.; Kladi, K. P.; Tsivintzelis, I.; Zuburtikudis, I.; Panayiotou, C. *Acta Biomaterialia* **2008,** *4*, 756.
8. Ludueña, L. N.; Alvarez, V. A.; Vazquez, A. *Mater. Sci. Eng. A* **2007,** *460–461*, 121.
9. Dubois, P.; Jacobs, C.; Jerome, R.; Teyssie, P. *Macromolecules* **1991,** *24*, 2266.
10. Kim, E. G.; Kim, B. S.; Kim, D. S. *J. Appl. Polym. Sci.* **2007,** *103*, 928.
11. Messersmith, P. B.; Giannelis, E. P. *J. Polym. Sci. Part A: Polym. Chem.* **1995,** *33*, 1047.
12. Kojima, Y.; Usuki, A.; Kawasumi, M.; Okada, A.; Fukushima, Y.; Kurauchi, T.; Kamigaito, O. *J. Mater. Res.* **1993,** *8*, 1185.
13. Gilman, J. W.; Jackson, C. L.; Morgan, A. B.; Harris, R.; Manias, E.; Giannelis, E. P.; Wuthenow, M.; Hilton, D.; Phillips, S. H. *Chem. Mater.* **2000, 12, 1866.**
14. Gorrasi, G.; Tortora, M.; Vittoria, V.; Pollet, E.; Lepoittevin, B.; Alexandre, M.; Dubois, P. *Polymer* **2003,** *44*, 2271.
15. Zhang, Z.; Yang, J.-L.; Friedrich, K. *Polymer* **2004,** *45*, 3481.
16. Lee, D. C.; Jang, L. W. *J. Appl. Polym. Sci.* **1996,** *61*, 1117.

17. Hasegawa, N.; Kawasumi, M.; Kato, M.; Usuki, A.; Okada, A. *J. Appl. Polym. Sci.* **1998,** *67*, 87.
18. Alexandre, M.; Dubois, P. *Mater. Sci. Eng. R: Rep.* **2000,** *28*, 1.
19. Chen, B.; Evans, J. R. G. *Macromolecules* **2006,** *39*, 747.
20. Maiti, P. *Langmuir* **2003,** *19*, 5502.
21. Matzinos, P.; Tserki, V.; Kontoyiannis, A.; Panayiotou, C. *Polym. Degrad. Stabil.* **2002,** *77*, 17.
22. Messersmith, P. B.; Giannelis, E. P. *Chem. Mater.* **1993,** *5*, 1064.
23. Fischer, H. *Mater. Sci. Eng. C* **2003,** *23*, 763.
24. Weon, J. I.; Sue, H. *J. Polymer* **2005,** *46*, 6325.
25. Ogata, N.; Jimenez, G.; Kawai, H.; Ogihara, T. *J. Polym. Sci. Part B: Polym. Phys.* **1997,** *35*, 389.
26. Krikorian, V.; Pochan, D. *J. Chem. Mater.* **2003,** *15*, 4317.
27. Janigová, I.; Lednický, F.; Mošková, D. J.; Chodák, I. *Macromol. Symposia* **2011,** *301*, 1.
28. Chen, B.; Evans, J. R. G. *Macromolecules* **2005,** *39*, 747.
29. Ratinac, K. R.; Gilbert, R. G.; Ye, L.; Jones, A. S.; Ringer, S. P. *Polymer* **2006,** *47*, 6337.
30. VanderHart, D. L.; Asano, A.; Gilman, J. W. *Macromolecules* **2001,** *34*, 3819.
31. VanderHart, D. L.; Asano, A.; Gilman, J. W. *Chem. Mater.* **2001,** *13*, 3796.
32. Yam, W. Y.; Ismail, J.; Kammer, H. W.; Schmidt, H.; Kummerlöwe, C. *Polymer* **1999,** *40*, 5545.
33. Di Franco, C. R.; Cyras, V. P.; Busalmen, J. P.; Ruseckaite, R. A.; Vázquez, A. *Polym. Degrad. Stabil.* **2004,** *86*, 95.
34. Alvarez, V.; Mondragón, I.; Vázquez, A. *Compos. Interfaces* **2007,** *14*, 605.
35. Su, S.; Wilkie, C. A. *Polym. Degrad. Stabil.* **2004,** *83*, 347.
36. Goulas, A. E.; Riganakos, K. A.; Kontominas, M. G. *Radiat. Phys. Chem.* **2004,** *69*, 411.
37. Labidi, S.; Azema, N.; Perrin, D.; Lopez-Cuesta, J.-M. *Polym. Degrad. Stabil.* **2010,** *95*, 382.
38. Nielsen, L. E.; Landel, R. F. Mechanical Properties of Polymers and Composites; Marcel Dekker: New York, **1994,** p 307.
39. Sun, L.; Gibson, R. F.; Gordaninejad, F.; Suhr J. *Compos. Sci. Technol.* **2009,** *69*, 2392.
40. Galeski, A. *Prog. Polym. Sci.* **2003,** *28*, 1643.
41. LeBaron, P. C.; Wang, Z.; Pinnavaia, T. *J. Appl. Clay Sci.* **1999,** *15*, 11.
42. Yano, K.; Usuki, A.; Okada, A. *J. Polym. Sci. Part A: Polym. Chem.* **1997,** *35*, 2289.
43. Yano, K.; Usuki, A.; Okada, A.; Kurauchi, T.; Kamigaito, O. *J. Polym. Sci. Part A: Polym. Chem.* **1993,** *31*, 2493.
44. Giannelis, E. P. *Adv. Mater.* **1996,** *8*, 29.
45. Strawhecker, K. E.; Manias, E. *Chem. Mater.* **2000,** *12*, 2943.
46. Fukushima, K.; Abbate, C.; Tabuani, D.; Gennari, M.; Rizzarelli, P.; Camino, G. *Mater. Sci. Eng. C* **2010,** *30*, 566.
47. Wu, T.; Xie, T.; Yang, G. *Appl. Clay Sci.* **2009,** *45*, 105.
48. Ratto, J. A.; Steeves, D. M.; Welsh, E. A.; Powell, B. E. 57th ANTEC'99, **1999,** p 1628.
49. Singh, N. K.; Purkayastha, B. D.; Roy, J. K.; Banik, R. M.; Yashpal, M.; Singh, G.; Malik, S.; Maiti, P. *ACS Appl. Mater. Interfaces* **2009,** *2*, 69.